

## Activities of Working Group Members and Colleagues

The following are ten contributions by members and colleagues of WG 32. Conclusions and Recommendations are then presented followed by five appendices that include the Working Group's Terms of Reference, membership, published literature related to WG 32 research, meeting reports and topic session/workshop summaries from PICES Annual Meetings, and article featured in PICES Press.

### *1. MaxEnt modelling of biogenic habitat-forming cold-water corals and sponges in the Northeast Pacific region of Canada*

Jackson W.F. Chu<sup>1</sup>, Jessica Nephin<sup>2</sup>, Samuel Georgian<sup>3</sup>, Anders Knudby<sup>4</sup>, Chris Rooper<sup>5</sup>, Katie S.P. Gale<sup>2</sup> and Janelle Curtis<sup>5</sup>

<sup>1</sup>Department of Ocean Sciences, Memorial University of Newfoundland, St. John's, Newfoundland and Labrador, Canada

<sup>2</sup>Fisheries and Oceans Canada, Institute of Ocean Sciences, Sidney, British Columbia, Canada

<sup>3</sup>Marine Conservation Institute, Seattle, Washington, USA

<sup>4</sup>Department of Geography, Environment and Geomatics, University of Ottawa, Ottawa, Ontario, Canada

<sup>5</sup>Fisheries and Oceans Canada, Pacific Biological Station, Nanaimo, British Columbia, Canada

#### Background and overview

This section summarizes the recent Canadian efforts in predictive modelling of the distributions of biogenic habitat-forming, cold-water corals and sponges (CWCS) in the Northeast Pacific region of Canada (NEPC). Biogenic habitat-forming CWCS are often the focal taxa when applying empirical frameworks designed to identify sensitive benthic areas or those that are vulnerable to significant adverse impacts as a result of fishing activities (Ardron *et al.*, 2014; Dunn *et al.*, 2014). These frameworks focus on criteria that can almost entirely be met by the presence of dense CWCS communities. Key ecosystem roles that CWCS have include habitat provisioning for early life history stages of rockfish and sharks (Baillon *et al.*, 2012; Henry *et al.*, 2013), nutrient cycling, and carbon sequestration (Henry and Roberts, 2007; Oevelen *et al.*, 2009; Chu and Leys, 2010; Chu *et al.*, 2011; Kahn *et al.*, 2015). Biological traits such as slow growth, low reproductive output and dispersal rates, and long life spans (Roark *et al.*, 2009; Jochum *et al.*, 2012) make CWCS especially vulnerable to destructive bottom contact fisheries. Thus, activities that remove or destroy CWCS directly results in the net loss of the aforementioned ecosystem functions and services.

Our NEPC case study area is the Pacific Exclusive Economic Zone (EEZ) of Canada. This region is notable for several globally unique biogenic habitat-forming CWCS communities (*e.g.*, glass sponge reefs, Krautter *et al.*, 2001) and is where the majority of Canadian seamounts are located (>80%, DFO,

2019). Seamount ecosystems are of noted interest to the scientific community because of their global biogeography patterns and high productivity. Dense populations of commercially important fish and communities of biogenic-habitat forming CWCS are frequently found at seamounts (Clark *et al.*, 2011; Guinotte and Davies, 2014). Historically, the majority of empirical knowledge on the distribution of habitat-forming CWCS in the NEPC has focused on the samples collected on the continental shelf and slope with only a sparse number of records coming from the offshore deep waters in the NEPC. Published knowledge of biogenic habitat-forming CWCS on NEPC seamounts has come from research mostly done at two outliers with summits occurring in <30 m depths (Bowie and Cobb seamounts); most seamounts in the NEPC do not have summits that extend into the epipelagic zone.

Species distribution models (SDMs) were developed for several major groupings of biogenic habitat-forming CWCS. The goals of these analyses were to assess the primary drivers of suitable habitat for CWCS in the NEPC, identify potential areas of high CWCS diversity (*i.e.*, areas that were suitable habitat for multiple CWCS groups), and determine the extent of CWCS suitable habitat at seamounts in this region. To assess areas as suitable habitat for multiple biogenic habitat-forming CWCS, a 'CWCS composite index' was created from combining spatial predictions from the individual models developed for each CWCS group. Several environmental data layers ( $n = 32$ ) were generated for SDM development; methods on how they were generated are described in detail. Additional details describe how historical CWCS occurrence records were queried and compiled from several regional databases and filtered before being used in SDM development. The CWCS composite index was applied to empirically assess seamounts that have been provisionally identified as ecologically significant habitats within the Canadian EEZ (Ban *et al.*, 2016).

## Data compilation

### *Environmental data layers*

SDMs require environmental data that cover the extent of the area of interest and are selected for their potential to influence the distribution of modelled taxa. Working Group 32 created an expansive set of 32, coarse-resolution (1 km<sup>2</sup>), environmental data layers for use in CWCS SDM development for the PICES convention area. These data layers were created following the methodology first described by Davies and Guinotte (2011) and since expanded upon by others (Guinotte and Davies, 2014; Rowden *et al.*, 2017; Georgian *et al.*, 2019). Variables were obtained from a variety of sources (Table 1.1) and cover a range of bathymetry-derived variables, physico-chemical variables, and water column properties that are useful in predicting the potential distributions of benthic species in major ocean basins elsewhere. This case study focused on the area that covers the EEZ of the NEPC.

Bathymetry data and their derivatives are ubiquitous in benthic SDM studies. For this study, bathymetric data ([https://topex.ucsd.edu/WWW\\_html/srtm30\\_plus.html](https://topex.ucsd.edu/WWW_html/srtm30_plus.html)) were obtained from the SRTM30+ layer at a native resolution of 0.0083° (~1 km) (Becker *et al.*, 2009; Sandwell *et al.*, 2014). The SRTM30+ layer (hereafter bathymetry) is derived from Sandwell *et al.* (2014), the Lamont-Doherty Earth Observatory Multibeam Synthesis Project, the JAMSTEC Data Site for Research Cruises, the National Center for Environmental Information (formerly the National Geophysical Data Center) Coastal Relief Model, and the International Bathymetric Chart of the Oceans.

**Table 1.1** Environmental data layers generated by WG 32 with associated data or methods reference.

Variable name	Unit	Native resolution	Reference
<i>Bathymetry-derived variables</i>			
Bottom depth	metres	0.0083°	Becker <i>et al.</i> , 2009; Sandwell <i>et al.</i> , 2014
Aspect – east-facing [ <i>eastness</i> ]*		0.0083°	Jenness, 2013a
Aspect – north-facing [ <i>northness</i> ]		0.0083°	Jenness, 2013a
Curvature – General [ <i>gencurve</i> ]		0.0083°	Jenness, 2013a
Curvature – Cross-Sectional [ <i>crosscurve</i> ]		0.0083°	Jenness, 2013a
Curvature – Longitudinal [ <i>longcurve</i> ]		0.0083°	Jenness, 2013a
Slope	degrees	0.0083°	Jenness, 2013a
Roughness [ <i>VRM</i> ]		0.0083°	Sappington <i>et al.</i> , 2007
Bathymetric Position Index [ <i>bpi</i> ] (1000m, 5000m, 10000m 20000m)		0.0083°	Jenness, 2013b
Seamounts polygon [ <i>seamounts</i> ]			Yesson <i>et al.</i> , 2011
<i>Chemical variables</i>			
Alkalinity	$\mu\text{mol l}^{-1}$	$3.6 \times 0.8\text{--}1.8^\circ$	Steinacher <i>et al.</i> , 2009
Dissolved inorganic carbon [ <i>DIC</i> ]	$\mu\text{mol l}^{-1}$	$3.6 \times 0.8\text{--}1.8^\circ$	Steinacher <i>et al.</i> , 2009
Omega - aragonite ( $\Omega_{\text{ARAG}}$ ) [ <i>arag</i> ]		$3.6 \times 0.8\text{--}1.8^\circ$	Steinacher <i>et al.</i> , 2009
Omega - calcite ( $\Omega_{\text{CALC}}$ ) [ <i>calc</i> ]		$3.6 \times 0.8\text{--}1.8^\circ$	Steinacher <i>et al.</i> , 2009
Dissolved oxygen [ <i>oxygen</i> ]	$\text{ml l}^{-1}$	1°	Garcia <i>et al.</i> , 2014a
Phosphate	$\mu\text{mol l}^{-1}$	1°	Garcia <i>et al.</i> , 2014b
Silicic acid [ <i>dSi</i> ]	$\mu\text{mol l}^{-1}$	1°	Garcia <i>et al.</i> , 2014b
Nitrate	$\mu\text{mol l}^{-1}$	1°	Garcia <i>et al.</i> , 2014b
Particulate organic carbon [ <i>POC</i> ]	$\text{g C m}^{-2} \text{yr}^{-1}$	0.05°	Lutz <i>et al.</i> , 2007
<i>Physical variables</i>			
Temperature	°C	0.25°	Locarnini <i>et al.</i> , 2013
Salinity	pss	0.25°	Zweng <i>et al.</i> , 2013
Current velocity – regional [ <i>regfl</i> ]	$\text{m s}^{-1}$	0.5°	Carton and Giese, 2008
Current velocity – vertical [ <i>vertfl</i> ]	$\text{m s}^{-1}$	0.5°	Carton and Giese, 2008
Current direction [ <i>curdir</i> ]	degrees	0.5°	Carton and Giese, 2008
Current direction – relative to aspect [ <i>curaspect</i> ]	degrees	0.5°	Rooper <i>et al.</i> , 2014
3D current-surface angle [ <i>curang</i> ]	degrees	0.5°	This study
<i>Surface-layer properties</i>			
Chlorophyll-a [ <i>chl-a</i> ]	$\text{mg m}^{-3}$	4 km	Aqua MODIS (NOAA)
Photosynthetically active radiation [ <i>PAR</i> ]	$\text{W m}^{-2}$	4 km	Aqua MODIS (NOAA)
Sea Surface Temperature [ <i>SST</i> ]	°C	4 km	Aqua MODIS (NOAA)

\* Shortened variable names are in square parentheses.

Several derivative variables were calculated from the bathymetry layer. Slope, aspect, and curvature were calculated using the toolkit ‘DEM Surface Tools v.2’ (Jenness, 2004, 2013a) for ArcGIS (v.10.4, ESRI). The slope of each grid cell (in degrees) was calculated using the four-cell method (Horn, 1981;

Jones, 1998). Aspect, or the maximum slope direction in degrees, is a circular variable (*i.e.*, the difference between 0° and 359° is one unit) and thus was converted into two components: north-facing aspect ( $\sin(\text{aspect})$ ) and east-facing aspect ( $\cos(\text{aspect})$ ). Curvature generally describes the shape of the seafloor as a proxy to how the water column can interact with the substratum. Three types of curvature were calculated: general curvature, cross-sectional curvature, and longitudinal curvature. For general curvature, convex features have more positive values and concave features are more negative. For cross-sectional curvature, positive values are indicative of local features that may induce water divergence, and negative values are indicative of features that induce water convergence. Longitudinal curvature assigns positive values to features where water velocity is expected to decrease and negative values to features where velocity is expected to increase.

### *Bathymetry*

Roughness is a measure of topographical complexity and was calculated using the vector ruggedness measure (VRM) index method (Sappington *et al.*, 2007). VRM generates a dimensionless index that incorporates the bathymetry, aspect and slope layers. This process uncouples the slope from the resulting roughness index calculated for a raster cell by measuring the dispersion of vectors orthogonal to the terrain surface for a user-defined neighbourhood of cells. Here, the VRM index layer was generated using a neighbourhood of the adjacent eight cells from the one km<sup>2</sup> bathymetry layer.

Bathymetric Position Index (BPI) quantifies the relative elevation of a feature relative to the surrounding seafloor, with positive values indicating features that are elevated and negative values indicating features that are depressed. BPI values close to zero indicate relatively flat surfaces or areas with constant slopes. As biological processes are scale-dependent, and because BPI is calculated at a user-defined scale, a range of BPI layers was generated: 1,000 m (the fine-scale limit of the method based on the bathymetry layer), 5,000 m, 10,000 m, and 20,000 m. BPI layers were generated using the toolkit ‘Land Facet Corridor Designer v1.2’ (Jenness, 2013b).

### *Oceanographic properties*

Data layers for temperature, salinity, dissolved oxygen, and several dissolved nutrients were generated from data obtained from the World Ocean Atlas (WOA, v.2 2013). Carbonate chemistry (dissolved inorganic carbon, total alkalinity,  $\Omega_{\text{ARAGONITE}}$ ,  $\Omega_{\text{CALCITE}}$ ) were obtained from Steinacher *et al.* (2009). Chlorophyll-a (chl-*a*), sea surface temperature (SST), and photosynthetically active radiation (PAR) data were generated using mission composites (average of 2002–2016 data) from the MODIS/Aqua NOAA program at a resolution of 4 km and resampled to match the extent and resolution of the bathymetry layer without interpolation.

Several layers that characterize current and flow patterns were generated because of the strong influence of water movement on sessile species distributions (Genin *et al.*, 1986; Leys *et al.*, 2011). A bottom current velocity layer was generated using data from the Simple Ocean Data Assimilation model (v.3.4.1, Carton and Giese, 2008) averaged as the composite of the years 1990–2007. Current velocities were calculated in both the horizontal and vertical dimensions, and current direction for each grid cell was calculated from zonal ( $u$ ) and meridional ( $v$ ) velocities according to the formula:

$$\text{Direction} = \frac{180}{\pi} \times \text{atan2}([u], [v]).$$

Current flows to the south when values are close to  $+180^\circ$  and  $-180^\circ$ , flows to the east at  $+90^\circ$ , flows to the west at  $-90^\circ$ , and flows to the north at  $0^\circ$ .

Two additional current layers were created to capture flow patterns relative to bathymetry. The first layer generated was a two-dimensional (2D) current layer that quantified current flow direction relative to seafloor aspect. In this 2D current layer, values of  $0^\circ$  indicate current flow is in the same direction as the direction of the steepest slope and values of  $180^\circ$  indicate current flows in the opposite direction of the steepest slope (*sensu* Rooper *et al.*, 2014). The second layer generated was a three-dimensional (3D) current layer that quantified the current direction relative to the seafloor plane. For this 3D current layer, the slope and aspect layers were used to define the 3D orientation of the seafloor for each raster cell, from which the direction normal to the plane was defined in Cartesian coordinates. The direction of the water current was then defined at the seafloor based on the velocities relative to the east-flowing ( $x$ ), north-flowing ( $y$ ), and vertical-flowing ( $z$ ) directions, and the angle between the two vectors was calculated. 3D current layer values near  $90^\circ$  indicate the current is flowing near-parallel to the seafloor and values less than  $90^\circ$  indicate current is flowing into the seafloor (*e.g.*, northward flowing current into a south-facing seafloor slope).

WOA, carbonate chemistry, and current data layers were transformed to match the extent and resolution of the bathymetry layer using a variable up-scaling approach that approximates conditions at the seafloor (Davies and Guinotte, 2011). Each layer was first interpolated to a slightly higher resolution ( $0.5^\circ$ ) than its native resolution using inverse distance weighting, resampled to match the extent and resolution of the bathymetry data, and draped over the bathymetry data within its depth range. WOA data were available as 102 depth-binned layers from depths of 0–5500 m. Vertical resolution of WOA depth layers were 5 m (from 0–100 m), 25 m (100–500 m), 50 m (500–2000 m), and 100 m (2000–5500 m). Carbonate chemistry data (Steinacher *et al.*, 2009) were available in 25 depth-binned layers (6, 19, 38, 62, 93, 133, 183, 245, 322, 415, 527, 661, 818, 1001, 1211, 1449, 1717, 2014, 2340, 2693, 3072, 3473, 3894, 4329, and 4775 m). Simple Ocean Data Assimilation (SODA) current data were available in 50 depth bins (5.0, 15.1, 25.2, 35.4, 45.6, 55.9, 66.3, 76.8, 87.6, 98.6, 110.1, 122.1, 134.9, 148.7, 164.1, 181.3, 201.3, 224.8, 253.1, 287.6, 330.0, 382.4, 446.7, 525.0, 618.7, 728.7, 855.0, 996.7, 1152.4, 1320.0, 1497.6, 1683.1, 1874.8, 2071.3, 2271.3, 2474.0, 2678.8, 2884.9, 3092.1, 3300.1, 3508.6, 3717.6, 3926.8, 4136.3, 4345.9, 4555.566, 4765.4, 4975.2, 5185.1, and 5395.0 m). This up-scaling approach has repeatedly been shown to be effective for many global and regional scale variables (Davies and Guinotte, 2011; Yesson *et al.*, 2012).

All data layers were projected in the world equidistant conic PICES azimuthal equidistance projection ( $-180$  central meridian, 1.0 km linear unit). The edges of data layers do not completely extend into the coastal fjords habitats in the NEPC. Thus this study could not capture this habitat type which is known to harbour dense populations of CWCS taxa (Leys *et al.*, 2004; Gasbarro *et al.*, 2018).

### *Species records*

While CWCS communities have been studied extensively in the NEPC, a comprehensive dataset of georeferenced occurrence records had not been compiled prior to this study. The majority of the CWCS records came from Fisheries and Oceans Canada (DFO) research and commercial catch databases. CWCS are recorded as incidental catch in the commercial databases. DFO research records spanned 1963–2017 and include targeted surveys for stock assessments of commercial invertebrate and groundfish populations and synoptic research bottom trawl surveys used for monitoring biogeographic areas within the Canadian EEZ. DFO commercial groundfish catch records include fisher and observer

logbooks and dockside validation data from trawl, trap, and longline fisheries throughout this region; only records from 1996–2017 were used in this study because of recording reliability (M. Surry, DFO pers. comm.). Queries of the DFO databases were done using internal, three-digit DFO codes ( $n = 581$ ) that uniquely identify CWCS taxa to varying taxonomic levels (*e.g.*, 2A0 = Porifera, 3S6 = *Paragorgia arborea*). Additional records up to 2014 were compiled from the Royal British Columbia Museum (RBCM) archives which are now available in open access (Wheeler, 2018).

Although over 17,900 individual CWCS records were compiled from the various data sources, additional data management and quality control and assurance steps were required before species data could be meaningfully used in SDMs. CWCS records spanned several decades and several levels of taxonomic resolution (*e.g.*, identified down to only phylum level or down to species level). Up-to-date taxonomic names and a complete taxonomic hierarchy were manually appended to records and verified in the World Register of Marine Species (Worms Editorial Board, 2018). *A priori* expert-knowledge guided parsing of the records in order to filter out records that were inappropriate for use in SDMs focused on biogenic habitat-forming marine CWCS. For example, fresh-water sponges (*e.g.*, *Spongila lacustris*) present in the museum records were filtered out based on expert-knowledge. Records of *Calcarea* class of sponges were excluded because no biogenic habitat-forming calcareous sponges occur in the NEPC. Because of the varying degrees of taxonomic resolution, only records with taxonomic resolution down to at least the class-level for sponges and order-level for corals were used in models. Records were pooled into six general biogenic habitat-forming CWCS groups. Four of these groups were orders of cold-water corals: Alcyonacea (soft corals), Scleractinia (stony corals), Antipatharia (black corals), and Pennatulacea (sea pens). We also modeled the distributions of two classes of sponges: Hexactinellida (glass sponges) and Demospongiae (demosponges) (Fig. 1.1).

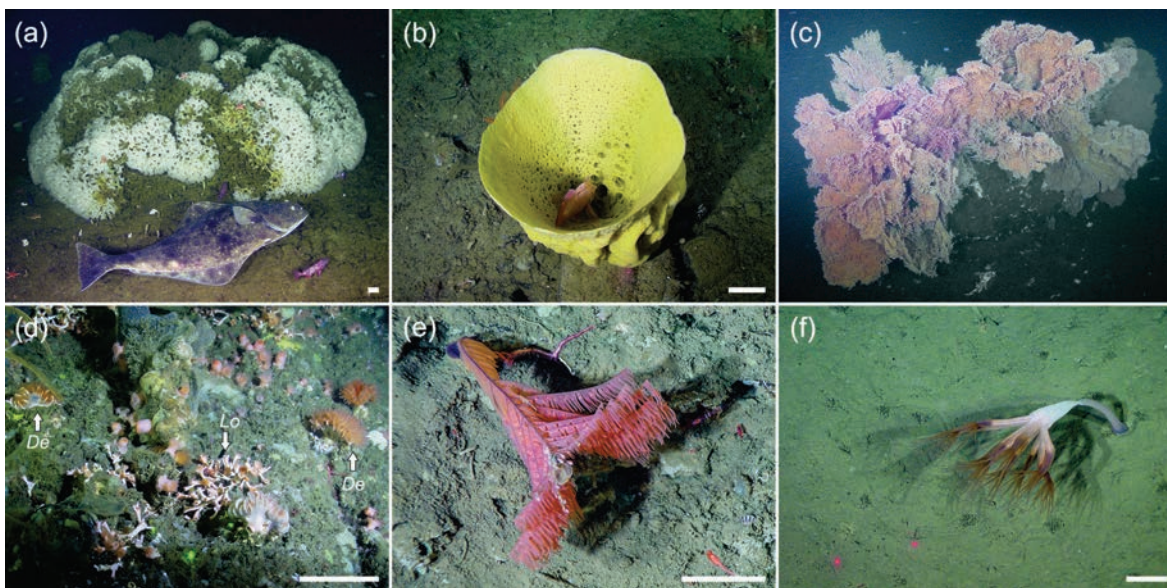


**Fig. 1.1** *In situ* examples of the major, biogenic habitat-forming cold-water coral and sponges from the Northeast Pacific Region of Canada. (a) Glass sponge *Farrea occa* (class Hexactinellida), (b) demosponge *Mycale loveni* (class Demospongiae), (c) soft coral *Primnoa pacifica* (order Alcyonacea); also a gorgonian coral. (d) Stony corals *Desmophyllum* sp. (De) and *Lophelia pertusa* (Lo) (order Scleractinia), (e) black coral *Bathypathes* sp. (order Antipatharia), (f) sea pen *Umbellula* sp. (order Pennatulacea). Scale bars: (a,b,d) 10 cm, (e,f) 5 cm. No scale bar was available for (c).

Historically, several families of biogenic habitat-forming corals were associated with the now-defunct order Gorgonacea. However, since it is still common to refer to these corals (now in the order Alcyonacea) as ‘gorgonians’, we created a gorgonian model by using a subset of records ( $n = 428$ ) in the ‘soft coral’ group that had at least a family-level of identification from the coral families: Anthothelidae, Paragorgiidae, Corallidae, Keroeididae, Acanthogorgiidae, Plexauridae, Gorgoniidae, Chrysogorgiidae, Primnoidae, and Isididae following the gorgonian grouping of Miyamoto *et al.* (2017). Sponge diversity and plasticity is problematic for species-level identification.

While the majority of glass sponges occurring in the NEPC are biogenic habitat-forming types, demosponges occupy niches that range from intertidal to deep-sea, with many species in this region being encrusting, non-habitat forming morphotypes. To prevent intertidal species from adding uncertainty to models developed for biogenic habitat-forming types, only demosponge records occurring in  $>100$  m depths were used in the models which improved the performance of the final models (Chu *et al.*, 2019).

Following Davies and Guinotte (2011), coral and sponge data for each group were gridded to the  $1 \text{ km}^2$  resolution of the environmental data layers and redundant records in each cell were removed (*i.e.*, only one presence record per cell per group). Table 1.2 summarizes the final number of records in each of the CWCS groups used in this study.

**Table 1.2** Number of records used in group-specific cold-water coral and sponge (CWCS) models.

CWCS group	Presence	Trawl-absences*	Depth-range** (m)
Glass sponges	1494	3248	28–3368
Demosponges	570	3465	100–2660
Soft corals	1960	4030	18–3624
Stony corals	717	4330	24–1388
Sea pens	3050	3678	8–2458
Black corals	51	4351	81–1985
Gorgonian corals	428	4447	41–3624

\* Trawl-absences were generated from synoptic trawl surveys. The shallow extent of demosponge records was truncated at 100 m to remove non-biogenic habitat-forming types (*e.g.*, encrusting intertidal spp.).

\*\* Depth-range is the observed depth of the presence records.

Note that the gorgonian coral presence records are a subset of the soft coral records.

## Species distribution modelling

### *Generating targeted absence data and depth masking*

Individual MaxEnt species distribution models were developed for the seven CWCS groups. MaxEnt is often used in study areas where data are limited to only species presence data. However, the predictive power of SDMs is increased with the knowledge of absence locations (Phillips *et al.*, 2009). Therefore, targeted absence data were generated by taking advantage of the DFO synoptic research trawl surveys that occur in the study area (Nottingham *et al.*, 2018) rather than using the random background

sampling method that is the default setting in MaxEnt. Since 2003, DFO has followed a depth-stratified, random sampling trawl design over the area spanning the extent of the presence records in this study (Fig. 1.2 a,b). Trawl surveys identify all species caught in a trawl. Thus those without the occurrence of any of the model-specific CWCS species codes were considered a targeted absence record (Table 1.2). DFO synoptic research trawl surveys have been fairly reliable when used to generate absence data in SDMs that require presence–absence species data (*e.g.*, Random Forest, Beazley *et al.*, 2018).

The combined CWCS presence records occupied a depth range of 8–3600 m which reflects the depths of potential fishing activity in the NEPC. Seamount species are characteristically distributed within a preferred depth range (Clark *et al.*, 2010). Therefore, the maximum modelled depth was limited to the depth range occupied by the presence records of each CWCS group (Table 1.2). MaxEnt (v.3.3.3e, Phillips *et al.*, 2010) models were run with the default parameters for the convergent threshold (1025), maximum iteration value (500), and regularization multiplier (1) using the R package ‘dismo’ (Hijmans *et al.*, 2017).

### *Environmental variable selection*

Although MaxEnt is reasonably robust to multicollinearity among environmental variables used as predictors of species distributions (Elith *et al.*, 2011), best SDM practices should always reduce the degree of correlation among model predictors. Using the R package ‘usdm’ (Naimi *et al.*, 2014), variance inflation factors (VIFs) were examined among environmental variables. Values of the environmental variables were extracted at the location of the species data and VIFs were calculated starting with the complete set of environmental data layers. Variables with the highest VIF were iteratively removed until the final set of variables all had VIF values <10. Ecophysiological relevant variables were preferentially retained (*e.g.*, silicic acid for sponge groups, carbonate chemistry variables for corals) rather than variables with no direct influence on organism physiology (*e.g.*, depth). This process of variable reduction was done separately using the species records belonging to each CWCS group. The final set of environmental variables used in each CWCS model is summarized in Table 1.3.

All models shared 18 variables: east-facing aspect, north-facing aspect, cross-sectional curvature, longitudinal curvature, slope, roughness, dissolved oxygen, regional current velocity, vertical current velocity, current direction, current direction relative to aspect, 3D current-surface angle, chlorophyll-a, photosynthetically active radiation, sea surface temperature, and topographic position index at three scales (1000 m, 5000 m, 20,000 m). The normalized relative importance for each variable used in their respective final CWCS models was assessed using a jack-knife procedure that compared models with and without the variable and the corresponding decrease in the area under the receiver operating characteristic curve (AUC, Phillips, 2005).

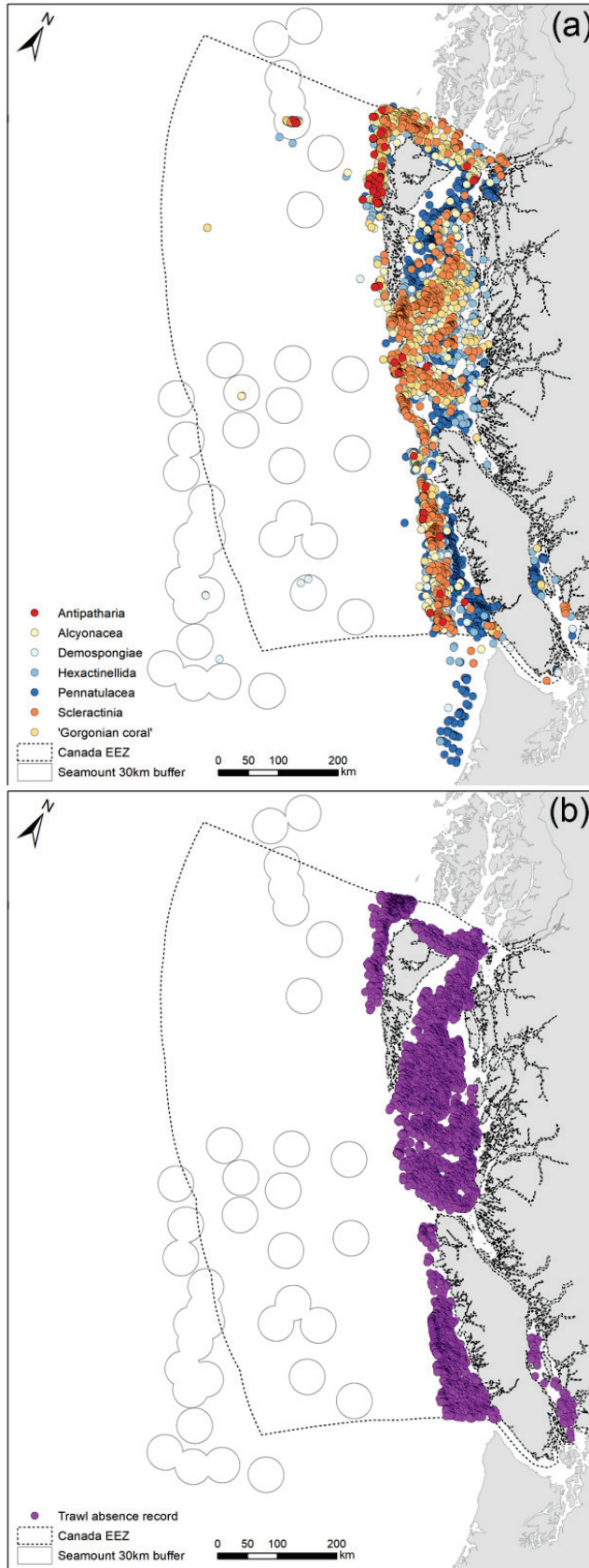


**Fig. 1.2** Biogenic habitat-forming cold-water coral and sponge (CWCS) records used in this study. (a) Presence records for six CWCS groups and the gorgonian coral subgroup. (b) Trawl absence records used in this study. Location of named seamounts are delineated by a 30 km buffer zone around their respective summits.

**Table 1.3** Final sets of environmental data layers used in models.

Variable	Glass sponges	Demo-sponges	Soft corals	Stony corals	Black corals	Sea pens	Gorgonian corals
<i>eastness</i>	X	X	X	X	X	X	X
<i>northness</i>	X	X	X	X	X	X	X
<i>crosscurve</i>	X	X	X	X	X	X	X
<i>longcurve</i>	X	X	X	X	X	X	X
<i>Slope</i>	X	X	X	X	X	X	X
<i>VRM</i>	X	X	X	X	X	X	X
<i>oxygen</i>	X	X	X	X	X	X	X
<i>Regfl</i>	X	X	X	X	X	X	X
<i>Vertfl</i>	X	X	X	X	X	X	X
<i>curdir</i>	X	X	X	X	X	X	X
<i>curaspect</i>	X	X	X	X	X	X	X
<i>curang</i>	X	X	X	X	X	X	X
<i>chl-a</i>	X	X	X	X	X	X	X
<i>PAR</i>	X	X	X	X	X	X	X
<i>SST</i>	X	X	X	X	X	X	X
<i>BPI1000</i>	X	X	X	X	X	X	X
<i>BPI5000</i>	X	X	X	X	X	X	X
<i>BPI20000</i>	X	X	X	X	X	X	X
<i>BPI10000</i>	X	X	X	X	X	X	–
<i>dSi</i>	X	X	–	X	X	–	–
<i>Arag</i>	–	X	–	X	X	–	–
<i>Calc</i>	–	–	X	–	–	X	X

Full name and units for each variable are summarized in Table 1.1.

### *Model validation*

Model performance was assessed using five-fold cross-validation where occurrence data (presence and absences) were randomly sampled to create five equal data partitions that follow the same data ratio of presence–absence. Models were trained on four folds and tested with the remaining fold. Each iteration of this procedure ( $n = 5$ ) rotated through the partitions always using a unique partition of records as the testing data. Mean and standard deviation of AUC, percentage correctly classified (PCC), correctly predicted presence (sensitivity), correctly predicted absence (specificity), and kappa was calculated to assess general model performance. Model thresholds were calculated by maximizing the sum and sensitivity using the R package ‘PresenceAbsence’ (Freeman and Moisen, 2008).

### *Model predictions of CWCS habitat suitability*

A bootstrap resampling procedure ( $n = 200$  iterations) was applied to each CWCS model to generate predictions of habitat suitability and spatially explicit measurements of uncertainty associated with the predictions at each raster cell (following Anderson *et al.*, 2016; Rowden *et al.*, 2017). Occurrence data and associated environmental predictors at those locations were randomly sampled with replacement to match the data ratio of presence and trawl-absences in Table 1.2. MaxEnt models were fit to each

iteration, and logistic predictions of habitat suitability (0–1) were generated with values close to one indicating more suitable habitat. Mean and standard deviation (SD) were calculated from the 200 predictions; we use SD to quantify the uncertainty of the model predictions (*i.e.*, predictions are more variable in areas with high SD).

In addition to generating predictions for each CWCS group, a ‘CWCS composite index’ was created that combined mean predictions among the four coral orders and two sponge class models. The gorgonian model outputs were excluded from the CWCS composite index because the species data were a subset of the Alyconacea model. Rasters of predicted habitat suitability for each CWCS group were reclassified into binary presence–absence layers using model-specific threshold (average of the five-folds) and then combined into a single, composite index (CI) layer where CI values of six would indicate suitable habitat for all six biogenic habitat-forming CWCS groups.

## Results and application

Based on the multiple evaluation metrics, CWCS MaxEnt models performed reasonably well (*e.g.*, AUC values ranged from 0.78–0.91, Table 1.4). *A priori* use of expert knowledge to parse the records was particularly effective as the Demospongiae model performance improved without shallow records (<100 m) when compared to a model that included shallow records (*e.g.*, AUC increased by ~0.6 and sensitivity increased by 0.11). Water column properties were generally the most important predictors for CWCS occurring in the study area (Table 1.5). All CWCS models shared dissolved oxygen ([O<sub>2</sub>]) as a top-3 ranked predictor based on relative importance (10–47%). Examination of the marginal response curves for [O<sub>2</sub>] indicates the probability of CWCS occurrence is inversely related to [O<sub>2</sub>] levels in the study area with maximum probability occurring at the lower [O<sub>2</sub>] distribution, or ~0.3 ml L<sup>-1</sup>. For both sponge groups, the top-ranked predictor was silicic acid (28–29%) with maximum probability occurring at the higher end of the silicic acid distribution or >100 μmol L<sup>-1</sup>. All CWCS models predict areas of high habitat suitability (HSI mean ~1) to occur in the NEPC although to varying extents (Fig. 1.3). Relative extent and locations of prediction uncertainty also varied but was generally low in predicted areas of high habitat suitability (Fig. 1.4).

**Table 1.4** Model performance statistics for cold-water coral and sponge MaxEnt models developed for this study.

CWCS group	AUC	Threshold	PCC	Sensitivity	Specificity	Kappa
Glass sponges	0.83 (0.01)	0.43 (0.02)	0.76 (0.02)	0.71 (0.05)	0.78 (0.05)	0.46 (0.03)
Demosponges	0.81 (0.02)	0.38 (0.06)	0.71 (0.06)	0.78 (0.11)	0.70 (0.09)	0.29 (0.05)
Soft corals	0.86 (0.01)	0.41 (0.04)	0.79 (0.02)	0.77 (0.06)	0.80 (0.05)	0.54 (0.02)
Stony corals	0.79 (0.01)	0.38 (0.05)	0.70 (0.05)	0.77 (0.08)	0.68 (0.07)	0.27 (0.04)
Black corals	0.91 (0.09)	0.31 (0.12)	0.97 (0.01)	0.84 (0.11)	0.97 (0.01)	0.39 (0.08)
Sea pens	0.78 (0.01)	0.57 (0.02)	0.71 (0.01)	0.70 (0.06)	0.71 (0.05)	0.41 (0.02)
Gorgonian corals	0.85 (0.01)	0.32 (0.06)	0.69 (0.03)	0.89 (0.04)	0.67 (0.04)	0.22 (0.03)

Values are mean ( $\pm 1$  SD) calculated from five cross-validation folds. AUC = Area Under the receiver operator characteristic Curve, PCC = percentage correctly classified.

**Table 1.5** Ranked environmental predictors based on normalized, permuted importance for variables used in cold-water coral and sponge MaxEnt models.

Rank	Glass sponges		Demosponges		Soft corals		Stony corals		Black corals		Sea pens		Gorgonian corals	
	Variable	%	Variable	%	Variable	%	Variable	%	Variable	%	Variable	%	Variable	%
1	<i>dSi</i>	28.0	<i>dSi</i>	29.9	<i>oxygen</i>	36.0	<i>oxygen</i>	20.6	<i>oxygen</i>	39.0	<i>oxygen</i>	29.0	<i>oxygen</i>	47.4
2	<i>oxygen</i>	17.4	<i>chl-a</i>	14.2	<i>calcite</i>	16.4	<i>SST</i>	16.2	<i>chl-a</i>	14.1	<i>chl-a</i>	13.4	<i>PAR</i>	13.7
3	<i>PAR</i>	12.8	<i>oxygen</i>	10.2	<i>SST</i>	15.7	<i>aragonite</i>	15.3	<i>VRM</i>	11.5	<i>SST</i>	11.9	<i>SST</i>	8.5
4	<i>regfl</i>	11.6	<i>northness</i>	6.6	<i>PAR</i>	11.8	<i>PAR</i>	13.4	<i>calcite</i>	8.7	<i>regfl</i>	10.0	<i>bpi20000</i>	7.2
5	<i>slope</i>	4.9	<i>slope</i>	6.5	<i>chl-a</i>	9.6	<i>dSi</i>	9.2	<i>SST</i>	6.7	<i>bpi20000</i>	8.3	<i>eastness</i>	4.1
6	<i>northness</i>	4.8	<i>curdir</i>	6.2	<i>VRM</i>	3.1	<i>verfl</i>	3.3	<i>eastness</i>	3.4	<i>slope</i>	5.8	<i>curdir</i>	3.6
7	<i>chl-a</i>	4.7	<i>curaspect</i>	5.6	<i>bpi20000</i>	2.1	<i>bpi5000</i>	3.2	<i>northness</i>	3.3	<i>calcite</i>	5.1	<i>regfl</i>	3.6
8	<i>VRM</i>	3.9	<i>PAR</i>	4.3	<i>eastness</i>	1.3	<i>curdir</i>	3.0	<i>dSi</i>	3.0	<i>PAR</i>	3.7	<i>northness</i>	2.9
9	<i>curdir</i>	3.7	<i>SST</i>	3.0	<i>northness</i>	1.1	<i>northness</i>	2.5	<i>slope</i>	2.4	<i>curaspect</i>	2.6	<i>chl-a</i>	2.7
10	<i>verfl</i>	2.0	<i>bpi20000</i>	2.9	<i>regfl</i>	1.0	<i>slope</i>	2.3	<i>Curaspect</i>	1.8	<i>northness</i>	2.5	<i>VRM</i>	2.0
11	<i>curaspect</i>	1.6	<i>eastness</i>	2.6	<i>slope</i>	0.6	<i>regfl</i>	2.1	<i>bpi20000</i>	1.5	<i>verfl</i>	2.4	<i>calcite</i>	1.8
12	<i>eastness</i>	1.3	<i>regfl</i>	2.3	<i>curaspect</i>	0.5	<i>eastness</i>	1.8	<i>curdir</i>	1.5	<i>eastness</i>	2.3	<i>slope</i>	0.8
13	<i>SST</i>	1.3	<i>bpi10000</i>	1.9	<i>verfl</i>	0.3	<i>bpi10000</i>	1.6	<i>longcurve</i>	1.0	<i>curdir</i>	2.2	<i>verfl</i>	0.6
14	<i>bpi20000</i>	1.2	<i>VRM</i>	1.3	<i>curdir</i>	0.3	<i>curaspect</i>	1.5	<i>regfl</i>	1.0	<i>bpi10000</i>	0.4	<i>curaspect</i>	0.4
15	<i>bpi10000</i>	0.7	<i>verfl</i>	0.9	<i>longcurve</i>	0.04	<i>chl-a</i>	1.2	<i>salinity</i>	0.4	<i>bpi5000</i>	0.1	<i>bpi5000</i>	0.2
16	<i>bpi5000</i>	0.2	<i>arag</i>	0.7	<i>bpi10000</i>	0.03	<i>bpi20000</i>	1.0	<i>bpi10000</i>	0.3	<i>curang</i>	0.08	<i>bpi1000</i>	0.1
17	<i>crosscurve</i>	0.04	<i>bpi5000</i>	0.4	<i>crosscurve</i>	0.01	<i>VRM</i>	0.9	<i>PAR</i>	0.2	<i>VRM</i>	0	<i>crosscurve</i>	0.1
18	<i>curang</i>	0.02	<i>longcurve</i>	0.4	<i>bpi5000</i>	0.01	<i>longcurve</i>	0.5	<i>crosscurve</i>	0.1	<i>bpi1000</i>	0	<i>curang</i>	0.01
19	<i>longcurve</i>	0	<i>curang</i>	0.1	<i>curang</i>	0.001	<i>curang</i>	0.4	<i>verfl</i>	0.1	<i>longcurve</i>	0	<i>longcurve</i>	0
20	<i>bpi1000</i>	0	<i>crosscurve</i>	0.05	<i>bpi1000</i>	0	<i>bpi1000</i>	0.2	<i>curang</i>	0.02	<i>crosscurve</i>	0	-	-
21	-	-	<i>bpi1000</i>	0.04	-	-	<i>crosscurve</i>	0.07	<i>bpi5000</i>	0.02	-	-	-	-
22	-	-	-	-	-	-	-	-	<i>bpi1000</i>	0	-	-	-	-

Full variable names are found in Table 1.1.

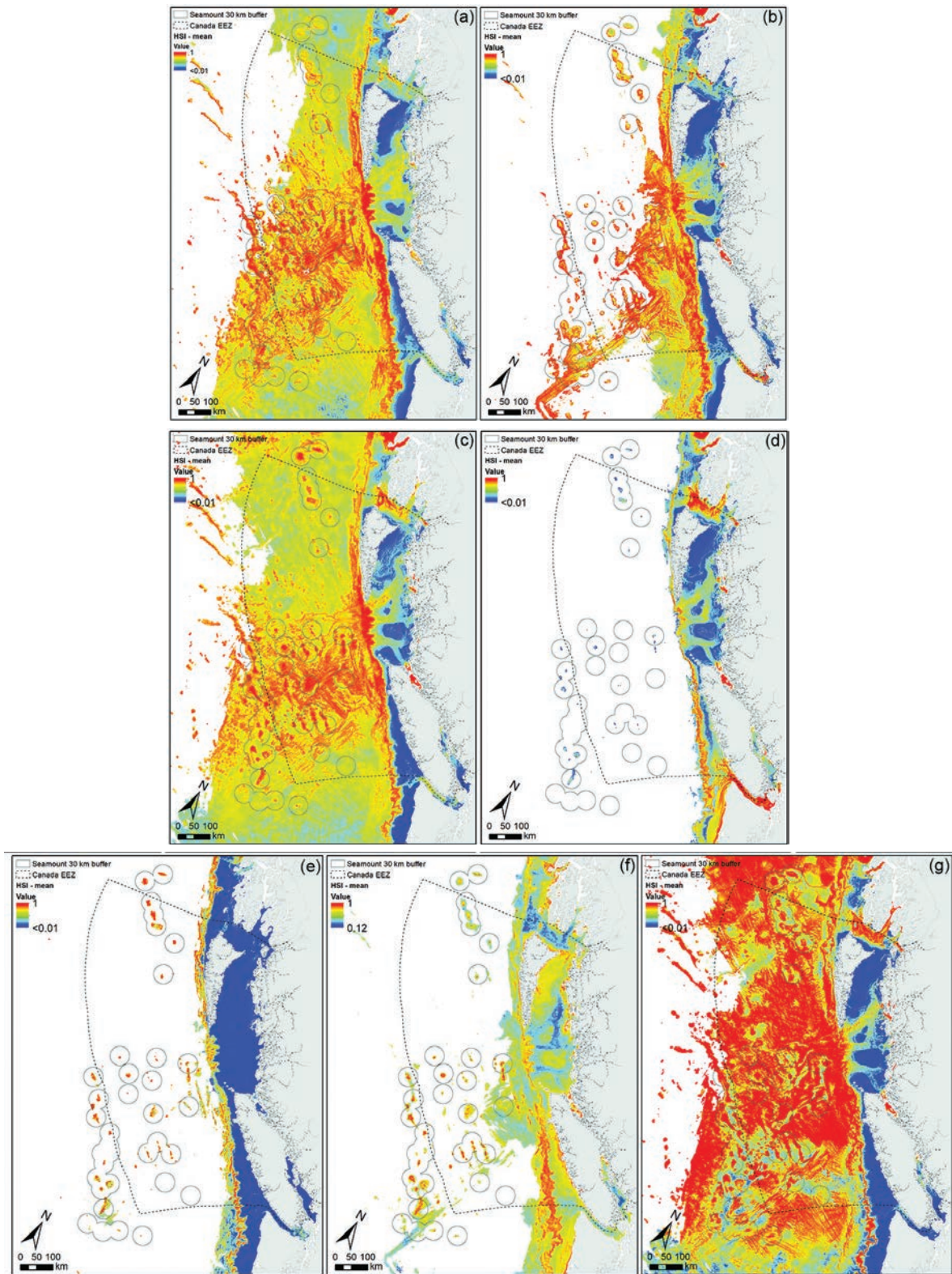


**Fig. 1.3** Means of predictions of habitat suitability index (HSI) for (a) Hexactinellida sponges, (b) Demospongiae sponges, (c) Alcyonacea corals, (d) Scleractinia corals, (e) Antipatharia corals, (f) Pennatulacea corals, and (g) Gorgonian corals.

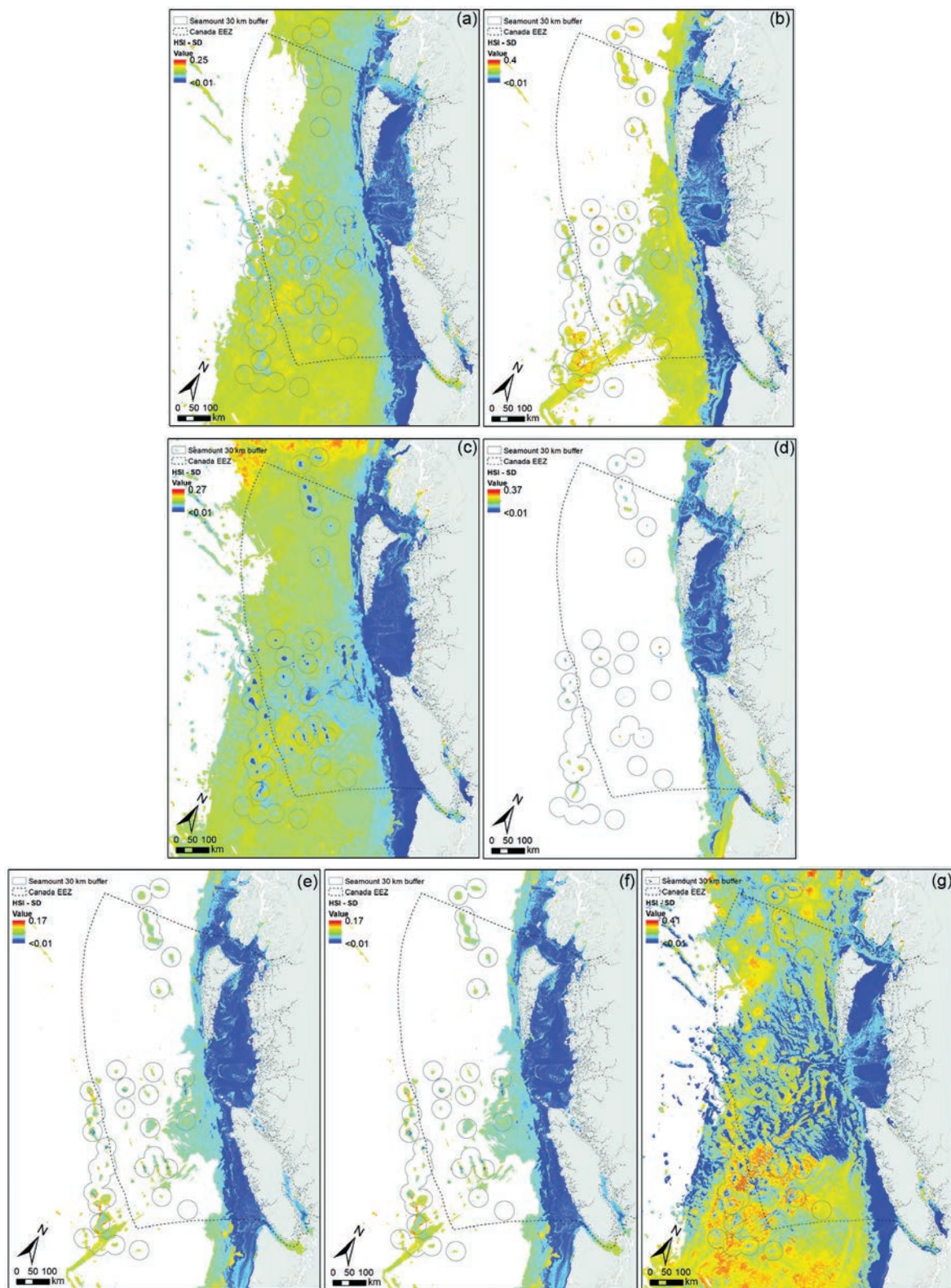


**Fig. 1.4** Standard deviation of predictions of habitat suitability index (HSI) for (a) Hexactinellida sponges, (b) Demospongiae sponges, (c) Alcyonacea corals, (d) Scleractinia corals, (e) Antipatharia corals, (f) Pennatulacea corals, and (g) Gorgonian corals.

The CWCS composite index resolved extensive areas of suitable habitat on the continental shelf and slope, between 500 and 1400 m bottom depths, for all six biogenic habitat-forming CWCS groups (index score = 6, Fig. 1.5). Smaller isolated patches with a composite index = 6 also occur at five seamounts (Bowie, Hodgkins, Oshawa, Dellwood, and Union) within the Canadian EEZ boundaries. If we combine the total area with a composite index value of  $\geq 5$ , 95% of the areas of potentially diverse biogenic habitat in the NEPC occurs on the continental shelf and slope of the study area (19,568 km<sup>2</sup>) with the remainder occurring on seamount and seamount-like features occurring in offshore waters (1,084 km<sup>2</sup>).

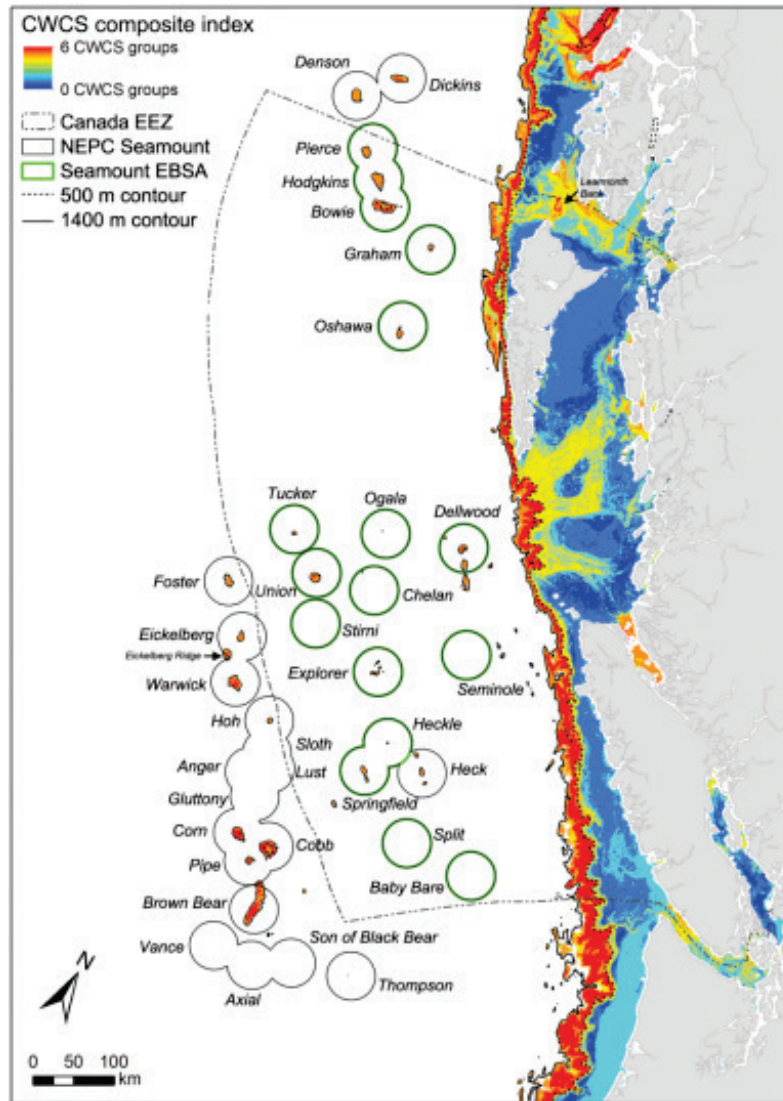


**Fig. 1.5** Composite index of areas of suitable habitat for multiple groups of biogenic habitat-forming cold-water corals and sponges (CWCS). Colour indicates areas of suitable habitat for multiple CWCS groups modelled in this study. Circles outline a 30 km radius buffer around the summits of named seamounts in the Northeast Pacific region of Canada (NEPC). Green highlighted circles are seamounts identified by Ban *et al.* (2016) as ecologically and biologically significant areas (EBSA). Contours delineate 500 m and 1400 m bottom depths which covers the majority of the area that is highly suitable habitat for a diversity of habitat-forming CWCS.

## Discussion and conclusions

This NEPC case study illustrates the value of species distribution models for assessing potentially important environmental variables that could influence the distributions of biogenic habitat-forming CWCS and generating habitat suitability predictions in areas with historically few observations (*e.g.*, offshore deep waters). Although there is variation in the level of importance among individual predictor variables included in each CWCS model, severely low [O<sub>2</sub>] ([O<sub>2</sub>] < 0.5 ml L<sup>-1</sup>) is an important predictor of habitat suitability for all CWCS groups in the NEPC (Chu *et al.*, 2019). Preliminary assessment of model predictions has validated the model prediction of severely low [O<sub>2</sub>] being a strong predictor of biogenic habitat-forming CWCS in the NEPC. Using underwater vehicles to perform *post-hoc* visual surveys guided by the model predictions, dense communities of CWCS were discovered at Union and Dellwood seamounts in [O<sub>2</sub>] < 0.2 ml L<sup>-1</sup> (Chu *et al.*, 2019). By combining multi-model outputs into a single CWCS composite index to represent biogenic habitat diversity, areas of suitable habitat for multiple CWCS can also be used to empirically assess areas that have been provisionally identified as candidates of conservation interest (*e.g.*, ecologically and biologically significant areas).

In addition to the importance of validating SDMs using *post-hoc* data collection, it is important to outline considerations when interpreting SDM outputs and how to apply them to facilitate future research directions. While oceanographic characteristics appeared to be the most important predictors in assessing CWCS habitat suitability, interpretations of results need to be constrained to scale, extent, and focal taxa of the study. Information on substratum type (*e.g.*, most CWCS require hard substratum) can influence CWCS recruitment and are often important predictors of CWCS distributions (Krigsman *et al.*, 2012; Masuda and Stone, 2015). However, these data were unavailable at the resolution and extent of the study area. Because most of the historical CWCS records in the NEPC have low taxonomic resolution, broad-scale models developed for this region require the available species data to be pooled into higher taxonomic groups. Although the regional models developed in this study still performed reasonably well, higher taxonomic resolution should generally improve model performance as this would account for species-specific niche differences which may spatially manifest in studies that focus on smaller scales.

In addition to improving overall data quality, applying different modelling approaches could also improve the degree of confidence ascribed to outputs and decrease the uncertainty associated with predictions generated using SDMs. Several different SDM approaches exist; aspects that differentiate models in their applied use include species input data requirements (*e.g.*, presence-only, presence-absence, abundance) and model-specific assumptions and uncertainty. Therefore, ensemble modelling could be a future step that assesses model-specific uncertainty (Araújo and New, 2007) by ‘averaging’ uncertainty among models similar to the forecasting approaches used in climatology (Rooper *et al.*, 2017). An additional modelling consideration could be to incorporate interspecific relationships into model assumptions (*e.g.*, Joint SDMs, Harris, 2015), thus modelling community-level habitat patterns while accounting for interactions among co-occurring species.

Because extensive sampling plans in logistically challenging environments are expensive, data will continue to be sparse in the immediate future. Assessing the distributions of biogenic habitat-forming CWCS is a precursor to understanding their role in the greater dynamics of the entire ecosystem (*e.g.*, biodiversity, ecosystem functioning, fisheries, *etc.*). In offshore areas where data are scant, data availability will likely remain poor given the remote setting and the complexities of international stakeholder dynamics. SDMs are one tool that can extrapolate modelled species–environment relationships into areas where species records are rare, thus providing an empirical foundation that can

promote hypothesis development which can, in turn, concentrate limited science resources into targeted data collection in logistically challenging environments (*e.g.*, Chu *et al.*, 2019).

## References

- Anderson, O.F., Guinotte, J.M., Rowden, A.A., Tracey, D.M., Mackay, K.A. and Clark, M.R. 2016. Habitat suitability models for predicting the occurrence of vulnerable marine ecosystems in the seas around New Zealand. *Deep-Sea Research Part I* **115**: 265–292.
- Araújo, M.B. and New, M. 2007. Ensemble forecasting of species distributions. *Trends in Ecology and Evolution* **22**: 42–47.
- Ardron, J.A., Clark, M.R., Penney, A.J., Hourigan, T.F., Rowden, A.A., Dunstan, P.K., Watling, L., Shank, T.M., Tracey, D.M., Dunn, M.R. and Parker, S.J. 2014. A systematic approach towards the identification and protection of vulnerable marine ecosystems. *Marine Policy* **49**: 146–154.
- Baillon, S., Hamel, J.F., Wareham, V.E. and Mercier, A. 2012. Deep cold-water corals as nurseries for fish larvae. *Frontiers in Ecology and the Environment* **10**: 351–356.
- Ban, S., Curtis, J.M.R., St. Germain, C., Perry, R.I. and Therriault, T.W. 2016. Identification of Ecologically and Biologically Significant Areas (EBSAs) in Canada's Offshore Pacific Bioregion. DFO Canadian Science Advisory Secretariat Research Document 2016/034, 152 pp.
- Beazley, L., Wang, Z., Kenchington, E., Yashayaev, I., Rapp, H.T., Xavier, J.R., Murillo, F.J., Fenton, D. and Fuller, S. 2018. Predicted distribution of the glass sponge *Vazella pourtalesi* on the Scotian Shelf and its persistence in the face of climatic variability. *PLoS ONE* **13**: e0205505, <https://doi.org/10.1371/journal.pone.0205505>.
- Becker, J.J., Sandwell, D.T., Smith, W.H.F., Braud, J., Binder, B., Depner, J., Fabre, D., Factor, J., Ingalls, S., Kim, S.-H., Ladner, R., Marks, K., Nelson, S., Pharaoh, A., Trimmer, R., Von Rosenberg, J., Wallace, G. and Weatherall, P. 2009 Global bathymetry and elevation data at 30 arc seconds resolution: SRTM30. *Marine Geodesy* **32**: 355–371.
- Carton, A. and Giese, B. 2008. A reanalysis of ocean climate using Simple Ocean Data Assimilation (SODA). *Monthly Weather Review* **136**: 2999–3017.
- Chu, J.W.F. and Leys, S.P. 2010. High resolution mapping of community structure in three glass sponge reefs (Porifera, Hexactinellida). *Marine Ecology Progress Series* **417**: 97–113.
- Chu, J.W.F., Maldonado, M., Yahel, G. and Leys, S.P. 2011. Glass sponge reefs as a silicon sink. *Marine Ecology Progress Series* **441**: 1–14.
- Chu, J.W.F., Nephin, J., Georgian, S., Knudby, A., Rooper, C. and Gale, K.S.P. 2019. Modelling the environmental niche space and distributions of cold-water corals and sponges in the Canadian northeast Pacific Ocean. *Deep-Sea Research Part I* **151**: 103063, <https://hdl.handle.net/10.1016/j.dsr.2019.06.009>.
- Clark, M.R., Rowden, A.A., Schlacher, T., Williams, A., Consalvey, M., Stocks, K.I., Rogers, A.D., O'Hara, T.D., White, M., Shank, T.M. and Hall-Spencer, J.H. 2010. The ecology of seamounts: Structure, function, and human impacts. *Annual Reviews of Marine Science* **2**: 253–278.
- Clark, M.R., Watling, L., Rowden, A.A., Guinotte, J.M. and Smith, C.R. 2011. A global seamount classification to aid the scientific design of marine protected area networks. *Ocean and Coastal Management* **54**: 19–36.
- Davies, A.J. and Guinotte, J.M. 2011. Global habitat suitability for framework-forming cold-water corals. *PLoS ONE* **6**: e18483, <https://doi.org/10.1371/journal.pone.0018483>.

- DFO (Fisheries and Oceans Canada). 2019. Biophysical and Ecological Overview of the Offshore Pacific Area of Interest (AOI). Canadian Science Advisory Secretariat Science Advisory Report, 2019/011.
- Dunn, D.C., Ardron, J., Bax, N., Bernal, P., Cleary, J., Cresswell, I., Donnelly, B., Dunstan, P., Gjerde, K., Johnson, D., Kaschner, K., Lascelles, B., Rice, J., von Nordheim, H., Wood, L. and Halpin, P.N. 2014. The Convention on Biological Diversity's Ecologically or Biologically Significant Areas: Origins, development, and current status. *Marine Policy* **49**: 137–145.
- Elith, J., Phillips, S.J., Hastie, T., Dudík, M., Chee, Y.E. and Yates, C.J. 2011. A statistical explanation of MaxEnt for ecologists. *Diversity and Distributions* **17**: 43–57.
- Freeman, E.A. and Moisen, G. 2008 PresenceAbsence: An R package for presence absence analysis. *Journal of Statistical Software* **23**: 1–31.
- Garcia, H.E., Locarnini, R.A., Boyer, T., Antonov, J., Baranova, O., Zweng, M., Reagan, J. and Johnson, D. 2014a. World Ocean Atlas 2013, Volume 3: Dissolved Oxygen, Apparent Oxygen Utilization, and Oxygen Saturation *in*: NOAA Atlas NESDIS 75 *edited by* S. Levitus. 27 pp.
- Garcia, H.E., Locarnini, R.A., Boyer, T.P., Antonov, J.I., Baranova, O.K., Zweng, M.M., Reagan, J.R. and Johnson, D.R. 2014b. World Ocean Atlas 2013, Volume 4: Dissolved Inorganic Nutrients (phosphate, nitrate, silicate) *in*: NOAA Atlas NESDIS 76 *edited by* S. Levitus. 25 pp.
- Gasbarro, R., Wan, D. and Tunnicliffe, V. 2018. Composition and functional diversity of macrofaunal assemblages on vertical walls of a deep northeast Pacific fjord. *Marine Ecology Progress Series* **597**: 47–64.
- Genin, A., Dayton, P.K., Lonsdale, P.F. and Spiess, F.N. 1986. Corals on seamount peaks provide evidence of current acceleration over deep-sea topography. *Nature* **322**: 59–61.
- Georgian, S.E., Anderson, O.F. and Rowden, A.A. 2019. Ensemble habitat suitability modeling of vulnerable marine ecosystem indicator taxa to inform deep-sea fisheries management in the South Pacific Ocean. *Fisheries Research* **211**: 256–274.
- Guinotte, J.M. and Davies, A.J. 2014. Predicted deep-sea coral habitat suitability for the U.S. West Coast. *PLoS ONE* **9**: e93918, <https://doi.org/10.1371/journal.pone.0093918>.
- Harris, D.J. 2015. Generating realistic assemblages with a joint species distribution model. *Methods in Ecology and Evolution* **6**: 465–473.
- Henry, L.A. and Roberts, J.M. 2007. Biodiversity and ecological composition of macrobenthos on cold-water coral mounds and adjacent off-mound habitat in the bathyal Porcupine Seabight, NE Atlantic. *Deep-Sea Research Part I* **54**: 654–672.
- Henry, L., Moreno, J., Hennige, S.J., Wicks, L.C., Vad, J. and Roberts, J.M. 2013. Cold-water coral reef habitats benefit recreationally valuable sharks. *Biological Conservation* **161**: 67–70.
- Hijmans, R.J., Phillips, S., Leathwick, J., Elith, J. and Hijmans, M.R.J. 2017. Package “dismo.” <ftp://ftp.gr.xemacs.org/mirrors/CRAN/web/packages/dismo/dismo.pdf>.
- Horn, B. 1981. Hill shading and the reflectance map. *Proceedings of the IEEE* **69**: 14–47.
- Jenness, J.S. 2004. Calculating landscape surface area from digital elevation models. *Wildlife Society Bulletin* **32**: 829–839.
- Jenness, J.S. 2013a. DEM Surface Tools for ArcGIS. *DEM Surface Tools*. <http://www.jennessent.com/downloads/DEM%20Surface%20Tools%20for%20ArcGIS.pdf>.
- Jenness, J.S. 2013b. Land Facet Corridor Designer. [http://www.jennessent.com/arcgis/land\\_facets.htm](http://www.jennessent.com/arcgis/land_facets.htm).

- Jochum, K.P., Wang, X., Vennemann, T.W., Sinha, B. and Müller, W.E.G. 2012. Siliceous deep-sea sponge *Monorhaphis chuni*: A potential paleoclimate archive in ancient animals. *Chemical Geology* **300**: 143–151.
- Jones, K.H. 1998. A comparison of algorithms used to compute hill slope as a property of the DEM. *Computers and Geosciences* **24**: 315–323.
- Kahn, A.S., Yahel, G., Chu, J.W.F., Tunnicliffe, V. and Leys, S.P. 2015. Benthic grazing and carbon sequestration by deep-water glass sponge reefs. *Limnology and Oceanography* **60**: 78–88.
- Krautter, M., Conway, K.W., Barrie, J.V. and Neuweiler, M. 2001. Discovery of a “Living Dinosaur”: Globally unique modern hexactinellid sponge reefs off British Columbia, Canada. *Facies* **44**: 265–282.
- Krigsman, L.M., Yoklavich, M.M., Dick, E.J. and Cochrane, G.R. 2012. Models and maps: predicting the distribution of corals and other benthic macro-invertebrates in shelf habitats. *Ecosphere* **3**: 1–16.
- Leys, S.P., Wilson, K., Holeton, C., Reiswig, H.M., Austin, W.C. and Tunnicliffe, V. 2004. Patterns of glass sponge (Porifera, Hexactinellida) distribution in coastal waters of British Columbia. *Marine Ecology Progress Series* **283**: 133–149.
- Leys, S.P., Yahel, G., Reidenbach, M.A., Tunnicliffe, V., Shavit, U., Henry, M. and Reiswig, H.M. 2011. The sponge pump: the role of current induced flow in the design of the sponge body plan. *PLoS ONE* **6**: e27787, <https://doi.org/10.1371/journal.pone.0027787>.
- Locarnini, R.A., Mishonov, A.V., Antonov, J.I., Boyer, T.P., Garcia, H.E., Baranova, O.K., Zweng, M.M., Paver, C.R., Reagan, J.R., Johnson, D.R., Hamilton, M. and Seidov, D. 2013. World Ocean Atlas 2013, Volume 1: Temperature *in*: NOAA Atlas NESDIS 73 *edited by* S. Levitus. 40 pp.
- Lutz, M.J., Caldeira, K., Dunbar, R.B. and Behrenfeld, M.J. 2007. Seasonal rhythms of net primary production and particulate organic carbon flux to depth describe the efficiency of biological pump in the global ocean. *Journal of Geophysical Research* **112**: C10011, DOI: 10.1029/2006JC003706.
- Masuda, M.M. and Stone, R.P. 2015 Bayesian logistic mixed-effects modelling of transect data: relating red tree coral presence to habitat characteristics. *ICES Journal of Marine Science* **72**: 2674–2683.
- Miyamoto, M., Kiyota, M., Hayashibara, T. and Nonaka, M. 2017. Megafaunal composition of cold-water corals and other deep-sea benthos in the southern Emperor Seamounts area, North Pacific Ocean. *Galaxea, Journal of Coral Reef Studies* **19**: 19–30.
- Naimi, B., Hamm, N., Groen, T., Skidmore, A. and Toxopeus, A. 2014. Where is positional uncertainty a problem for species distribution modelling. *Ecography* **37**: 191–203.
- NASA Goddard Space Flight Center, Ocean Ecology Laboratory, Ocean Biology Processing Group. 2014. *Aqua Modis*. Greenbelt, MD, USA, <https://oceancolor.gsfc.nasa.gov/data/aqua/>.
- Nottingham, M.K., Williams, D.C., Wyeth, M.R. and Olsen, N. 2018. Summary of the West Coast Haida Gwaii Synoptic Bottom Trawl Survey, August 24 – September 19, 2012. Canadian Manuscript Report of Fisheries and Aquatic Sciences, 3133, pp. 1–55.
- Oevelen, D. van, Duineveld, G., Lavaleye, M., Mienis, F., Soetaert, K. and Heip, C.H.R. 2009. The cold-water coral community as hotspot of carbon cycling on continental margins: A food-web analysis from Rockall Bank (northeast Atlantic). *Limnology and Oceanography* **54**: 1829–1844.
- Phillips, S.J. 2005. A brief tutorial on Maxent. AT&T Research.
- Phillips, S.J., Dudík, M., Elith, J., Graham, C.H., Lehmann, A., Leathwick, J. and Ferrier, S. 2009. Sample selection bias and presence-only distribution models: Implications for background and pseudo-absence data. *Ecological Applications* **19**: 181–197.

- Roark, E.B., Guilderson, T.P., Dunbar, R.B., Fallon, S.J. and Mucciarone, D.A. 2009. Extreme longevity in proteinaceous deep-sea corals. *Proceedings of the National Academy of Sciences of the United States of America* **106**: 5204–5208.
- Rooper, C.N., Zimmermann, M., Prescott, M.M. and Hermann, A.J. 2014. Predictive models of coral and sponge distribution, abundance and diversity in bottom trawl surveys of the Aleutian Islands, Alaska. *Marine Ecology Progress Series* **503**: 157–176.
- Rooper, C.N., Zimmermann, M. and Prescott, M.M. 2017. Comparison of modeling methods to predict the spatial distribution of deep-sea coral and sponge in the Gulf of Alaska. *Deep-Sea Research Part I* **126**: 148–161.
- Rowden, A.A., Anderson, O.F., Georgian, S.E., Bowden, D.A., Clark, M.R., Pallentin, A. and Miller, A. 2017. High-resolution habitat suitability models for the conservation and management of vulnerable marine ecosystems on the Louisville Seamount Chain, South Pacific Ocean. *Frontiers in Marine Science* **4**: (335), <https://doi.org/10.3389/fmars.2017.00335>.
- Sandwell, D.T., Müller, R.D., Smith, H.F., Garcia, E. and Francis, R. 2014. New global marine gravity model from CryoSat-2 and Jason-1 reveals buried tectonic structure. *Science* **346**: 65–67.
- Sappington, J.M., Longshore, K.M. and Thompson, D.B. 2007. Quantifying landscape ruggedness for animal habitat analysis: A case study using bighorn sheep in the Mojave Desert. *The Journal of Wildlife Management* **71**: 1419–1426.
- Steinacher, M., Joos, F., Frolicher, T.L., Plattner, C.K. and Doney, S.C. 2009. Imminent ocean acidification in the Arctic projected with the NCAR global coupled carbon cycle-climate model. *Biogeosciences* **6**: 515–533.
- Wheeler, E. 2018. Royal BC Museum - Invertebrates Collection. v1.1. Royal British Columbia Museum. Dataset/Occurrence, <https://doi.org/10.5886/zh7n1e>.
- Worms Editorial Board. 2018. World Register of Marine Species. <http://www.marinespecies.org/>.
- Yesson, C., Clark, M.R., Taylor, M.L. and Rogers, A.D. 2011. The global distribution of seamounts based on 30 arc seconds bathymetry data. *Deep-Sea Research Part I* **58**: 442–453.
- Yesson, C., Taylor, M.L., Tittensor, D.P., Davies, A.J., Guinotte, J., Baco, A., Black, J., Hall-Spencer, J.M. and Rogers, A.D. 2012. Global habitat suitability of cold-water octocorals. *Journal of Biogeography* **39**: 1278–1292.
- Zweng, M.M., Reagan, J.R., Antonov, J.I., Locarnini, R.A., Mishonov, A.V., Boyer, T.P., Garcia, H.E., Baranova, O.K., Johnson, D.R., Seidov, D. and Biddle, M.M. 2013. World Ocean Atlas 2013, Volume 2: Salinity *in*: NOAA Atlas NESDIS 74 *edited by* S. Levitus. 39 pp.